Electronic Supplementary Information for:

Effects of the non-covalent interactions on the electronic and electrochemical properties of Cu(I) biquinoline complexes

Natalia P. Martínez,[a] Mauricio Isaacs,[a,b,c,] Allen G. Oliver,[d] G. Ferraudi,[d,e] A. Graham Lappin,[d*] Juan Guerrero.[f*]

[a]Facultad de Química, Pontificia Universidad Católica de Chile, Vicuña Mackenna 4860, 7820436 Macul, Santiago, Chile.
[b]Centro de Investigación en Nanotecnología y Materiales Avanzados CIEN-UC, Pontificia Universidad Católica de Chile, Chile.
[c]UC-Energy Research Center, Pontificia Universidad Católica de Chile, Chile.
[d]Department of Chemistry & Biochemistry, University of Notre Dame, Notre Dame, IN 46556-5670, USA.
E-mail: alexander.g.lappin.1@nd.edu
[e]Radiation Laboratory, University of Notre Dame, Notre Dame, IN 46556-5670, USA.
[f]Facultad de Química y Biología, Universidad de Santiago de Chile, Libertador Bernardo O'Higgins 3363, Estación central, Santiago, Chile.
E-mail: juan.guerrero@usach.cl

Table of contents

1. X-Ray Diffraction

Table S1. Crystal data and structure refinement for {[Cu^{I}(*biq*)$_2$]ClO_4-*biq*} (**1**) and [Cu(*biq*)$_2$]ClO_4 (**2**).

Comentado [NMA1]: Highlights text have been changed

Empirical formula	**$C_{54}H_{36}ClCuN_6O_4$ (1)**		**$C_{72}H_{53}Cl_2Cu_2N_8O_{10.50}$**	
Formula weight	931.88		1396.20	
Temperature	120(2) K		120(2) K	
Wavelength	0.71073 Å		0.71073 Å	
Crystal system	Monoclinic		Monoclinic	
Space group	P2/n		$P2_1$	
Unit cell dimensions	*a* = 13.7519(7) Å	α = 90°	a = 14.1241(11) Å	α = 90°
	b = 10.7132(6) Å	β = 97.732(2)°	b = 14.4166(11) Å	β = 103.416(3)°
	c = 14.1096(7) Å	γ = 90°	c = 15.9927(13) Å	γ = 90°
Volume	2059.82(19) $Å^3$		3167.6(4) $Å^3$	
Z	2		2	
Density (calculated)	1.502 $g.cm^{-3}$		1.464 $g.cm^{-3}$	
Absorption coefficient (μ)	0.655 mm^{-1}		0.826 mm^{-1}	
F(000)	960		1434	
Crystal color, habit	red, block		orange, plate	
Crystal size	0.238 × 0.142 × 0.110 mm^3		0.496 × 0.236 × 0.215 mm^3	
θ range for data collection	1.901 to 28.372°		1.309 to 27.254°	
Index ranges	-18 ≤ h ≤ 18, -14 ≤ k ≤ 14, -13 ≤ l ≤ 18		-18 ≤ h ≤ 13, -18 ≤ k ≤ 18, -19 ≤ l ≤ 20	
Reflections collected	23184		50518	
Independent reflections	5155 [R_{int} = 0.0333]		14099 [R_{int} = 0.0265]	
Completeness to θ = 25.242°	100.0 %		99.9 %	
Absorption correction	Numerical		Numerical	
Max. and min. transmission	0.9778 and 0.9002		0.9075 and 0.7884	
Refinement method	Full-matrix least-squares on F^2		Full-matrix least-squares on F2	
Data / restraints / parameters	5155 / 0 / 299		14099 / 1 / 854	
Goodness-of-fit on F^2	1.019		1.030	
Final R indices [I>2σ(I)]	R_1 = 0.0371, wR_2 = 0.0862		R_1 = 0.0388, wR_2 = 0.1078	
R indices (all data)	R_1 = 0.0531, wR_2 = 0.0929		R_1 = 0.0446, wR_2 = 0.1114	
Extinction coefficient	n/a		0.014(3)	
Largest diff. peak and hole	0.637 and -0.452 $e^-.Å^{-3}$		n/a	
Absolute structure parameter			0.925 and -0.688 $e^-.Å^{-3}$	

Table S2. Significant O…O contacts (Å)

Comentado [NMA2]: Highlights text have been changed

O1W	O8	2.924(8)
O2W	O4W[i]	2.70(2)
O3W	O4W	2.78(2)
O3W	O1	3.328(14)
O4W	O4	3.30(2)
O4W	O2W[ii]	2.70(2)
O4W	O5W	2.56(3)

Symmetry code: (i) –*x*+1, *y*+1/2, -*z*; (ii) –*x*+1, *y*-1/2, -*z*

2. Nuclear Magnetic Resonance

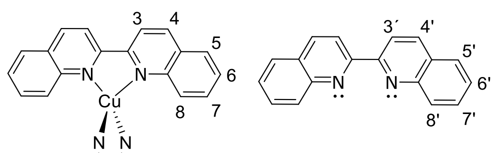

Fig. S1 Structure and labeling of protons in coordinated and free 2,2´-biquinoline in $[Cu(biq)_2]ClO_4$ complex.

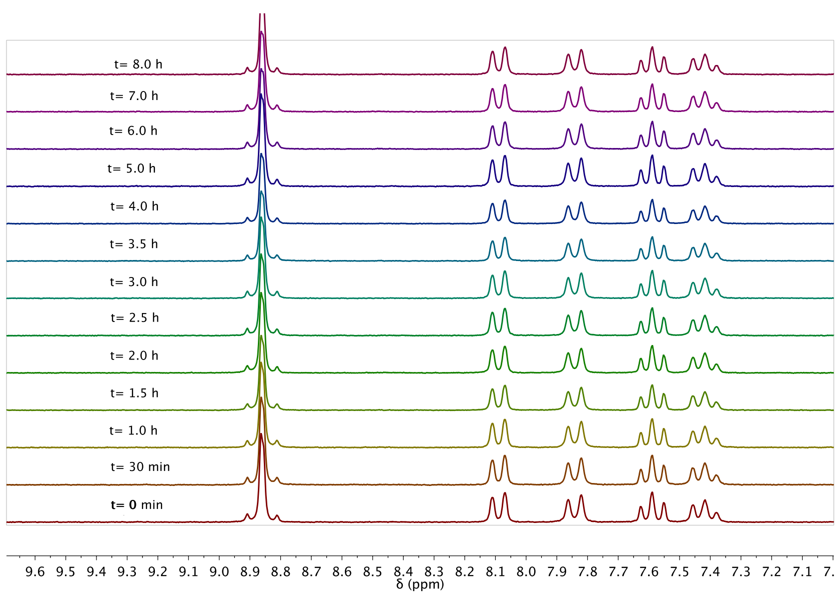

Fig. S2 Structural stability by 8 hours of complex $[Cu(biq)_2]ClO_4$ in CD_3CN at room temperature.

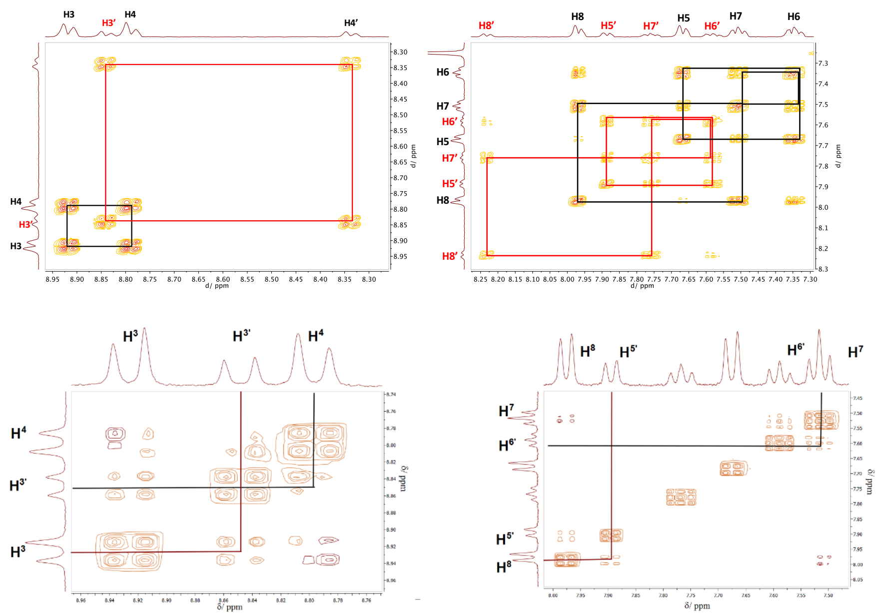

Fig. S3 Top: ^{1}H–^{1}H 2D-COSY spectra and of {[Cu^{I}(*biq*)$_2$]ClO$_4$-*biq*}. Bottom: 2D-NOESY interaction spectra of {[Cu^{I}(*biq*)$_2$]ClO$_4$-*biq*}. All measures in CDCl$_3$ at 300K.

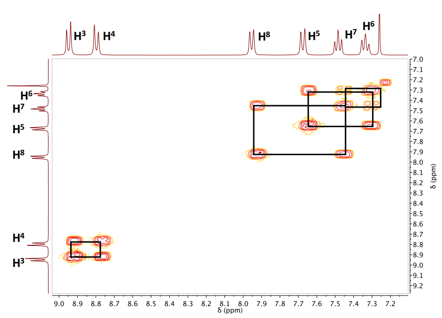

Fig. S4 ^{1}H–^{1}H 2D-COSY spectra of [Cu(*biq*)$_2$]ClO$_4$ in CDCl$_3$ at room temperature.

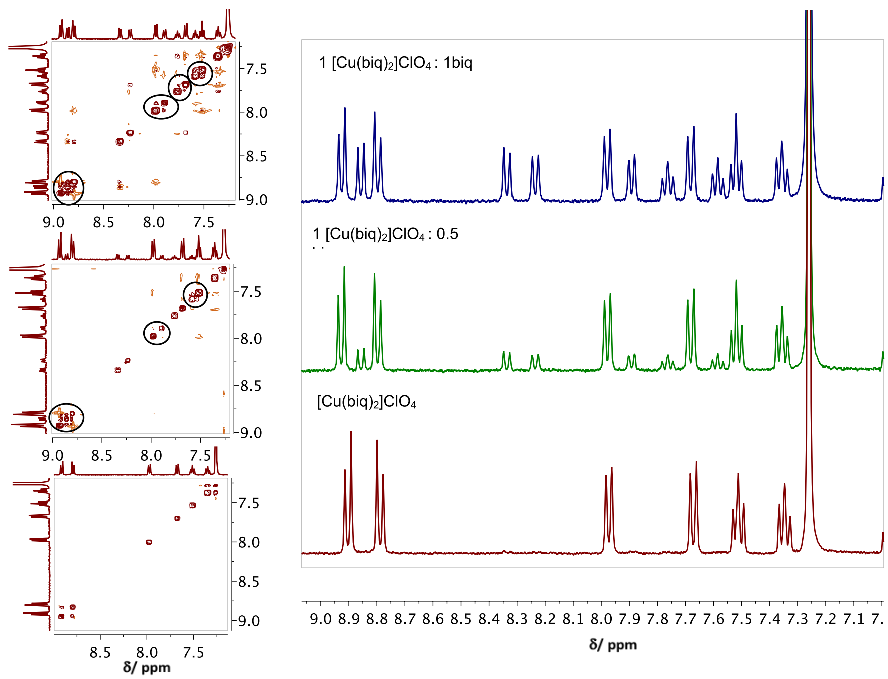

Fig. S5 ^{1}H-NMR spectra of [Cu^{I}(*biq*)$_2$]ClO_4 and titration with different relation of *biq* in CD_3Cl. Insert: NOESY spectra for every proton spectrum showed.

The NOESY experiments in chloroform show that formation of the adduct occurs even at a low amount of *biq* added to [Cu^{I}(*biq*)$_2$]ClO_4, i.e molar ratio 1[Cu^{I}(biq)$_2$]ClO_4:0.5 biq.

Comentado [NMA3]: New Figure added to S.I.
Old fig. S5 has been improved and added to corrected manuscript.

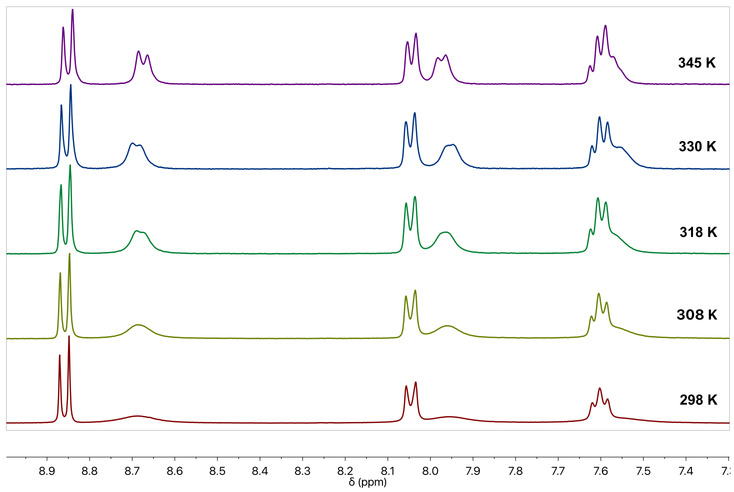

Fig. S5 ^{1}H-NMR spectra of variable temperature study (298 – 345 K) of {[Cu^{I}(*biq*)$_2$]ClO$_4$-*biq*} in CD_3CN.

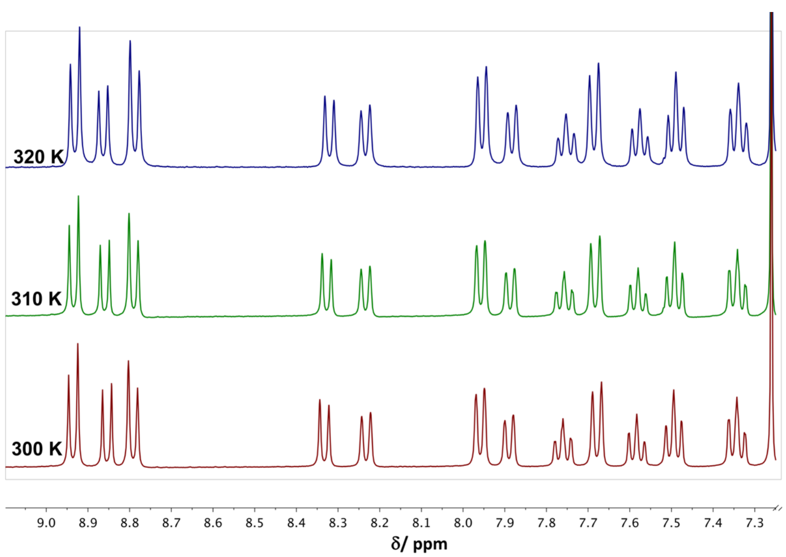

Fig. S7 ^{1}H-NMR spectra of variable temperature study (300 – 320 K) of {[Cu^{I}(*biq*)$_2$]ClO$_4$-*biq*}, 3.49 x 10^{-4} M in CD_3Cl. No perceptible shifting in signal frequency was observed.

Comentado [NMA4]: New Figure added to S.I.

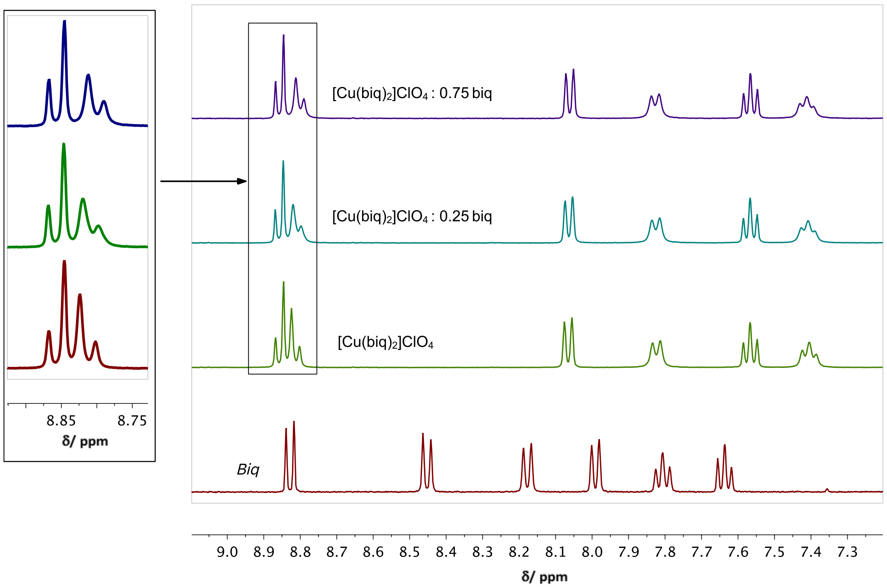

Fig. S8. ^{1}H-NMR spectra of *biq*, [Cu^I(*biq*)$_2$]ClO_4 and titration with different relation of *biq* in CD_3CN.

Comentado [NMA5]: New Figure added to S.I.

A broadening of the line shapes of protons signals, but not duplication of signals is observed after small amounts of *biq* is added to [Cu^I(*biq*)$_2$]ClO_4 in acetonitrile at 300 K, this is in agreement with an intermediate rate for *biq* exchange relative to the NMR time scale as observed for {[Cu^I(*biq*)$_2$]ClO_4-*biq*} in acetonitrile

Table S3. ^{1}H NMR data of the 2,2’-biquinoline and complexes $[Cu^{I}(biq)_2]ClO_4$ and $\{[Cu^{I}(biq)_2]ClO_4\text{-}biq\}$; δ/ppm, J/Hertz.

CDCl₃												
Proton	$H_{3'}$	$H_{4'}$	$H_{5'}$	$H_{6'}$	$H_{7'}$	$H_{8'}$	H_3	H_4	H_5	H_6	H_7	H_8
Biquinoline free	8.86 (d),2H	8.33 (d),2H	7.89 (d),2H	7.58 (t),2H	7.76 (t),2H	8.24 (d),2H	_	_	_	_	_	_
$[Cu^{I}(biq)_2]ClO_4$	_	_	_	_	_	_	8.95 (d),4H $J_{3\text{-}4}$=8.9	8.80 (d),4H	7.68 (d),4H $J_{5\text{-}6}$=7.5	7.34 (t),4H	7.48 (t),4H $J_{7\text{-}6}$=7.39	7.95 (d),4H $J_{8\text{-}7}$=7.7
$\{[Cu^{I}(biq)_2]ClO_4\text{-}biq\}$	8.85 (d),2H $J_{3'\text{-}4'}$=8.7	8.34 (d),2H	7.90 (d),2H $J_{5'6'}$=7.7	7.59 (t),2H $J_{7'\text{-}6'}$=7.7	7.77 (t),2H $J_{8'\text{-}7'}$=8.0	8.24 (d),2H	8.93 (d),4H $J_{3\text{-}4}$=8.9	8.90 (d),4H	7.68 (d),4H $J_{5\text{-}6}$=7.5	7.35 (t),4H $J_{7\text{-}6}$=7.4	7.52 (t),4H $J_{8\text{-}7}$=7.7	7.98 (d),2H
CD_3CN												
Proton	$H_{3'}$	$H_{4'}$	$H_{5'}$	$H_{6'}$	$H_{7'}$	$H_{8'}$	H_3	H_4	H_5	H_6	H_7	H_8
$[Cu^{I}(biq)_2]ClO_4$	_	_	_	_	_	_	8.87 (d),4H	8.83 (d),4H	7.81 (d),4H	7.39 (t),4H	7.57 (t),4H	8.07 (d),4H
$\{[Cu^{I}(biq)_2]ClO_4\text{-}biq\}$	_	_	_	_	_	_	8.85 (d),4H	8.68 (d),4H broad	7.94 (d),4H broad	7.54 4H weak	7.59 (t),4H	8.04 (d),4H

**Nomenclature NMR*: s= singlet; d= doublet; t=triplet.

3. Cyclic voltammetry

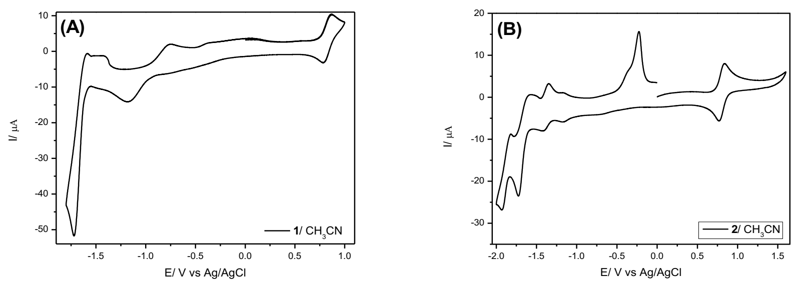

Fig. S9 Cyclic voltammogram of complex {[Cu^{I}(*biq*)$_2$]ClO_4-*biq*} (A) and [Cu^{I}(*biq*)$_2$]ClO_4 (B) to 100 mV/s in acetonitrile.

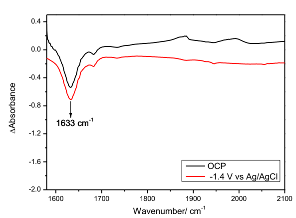

Fig. S10 IR-SEC of [Cu^{I}(*biq*)$_2$]ClO_4. Conditions: CD_3CN solution (1.00 x 10^{-4} M), FT-IR Nicolet iS10 spectrometer.

4. UV-Visible spectroscopy

Table S4. Summary of UV-visible data

Solvent		UV-Vis [λ (nm)]		
		Charge transfer MLCT/ nm	Molar extintion ε/ $M^{-1}cm^{-1}$	ligand centered (π – π*) (ε $M^{-1}cm^{-1}$)
CH_2Cl_2	{[Cu^{I}(*biq*)$_2$]ClO_4-*biq*}	549		206.5, 225, 258, 337.5, 325, 313, 300(s)
	[Cu^{I}(*biq*)$_2$]ClO_4	549	4.0 x 10^3	207.5, 259, 285(s). 298.3, 313.5, 326.6, 338.5, 357
ACN	{[Cu^{I}(*biq*)$_2$]ClO_4-*biq*}	549		235, 352, 393 (s)
	[Cu^{I}(*biq*)$_2$]ClO_4	549	5.5 x 10^3	223, 248, 338, 355, 387(s)

Comentado [NMA6]: Values for ε, was eliminated, because in the corrected manuscript we said that "cannot be determined accurately"

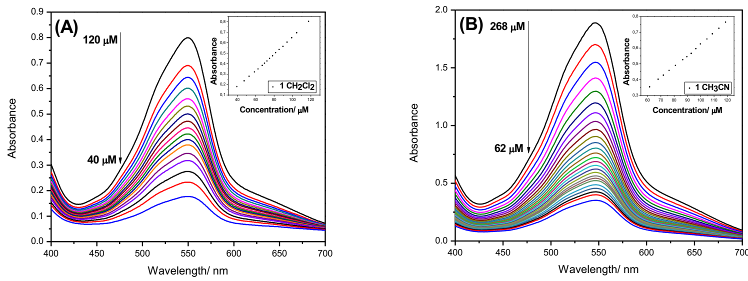

Fig. S11 UV-Vis spectra of solutions at different concentrations of {[Cu^{I}(*biq*)$_2$]ClO$_4$-*biq*}. Inset: a plot of the absorbance vs concentration for the range of concentrations shown in the picture. (A) in CH_2Cl_2, (B) in CH_3CN.

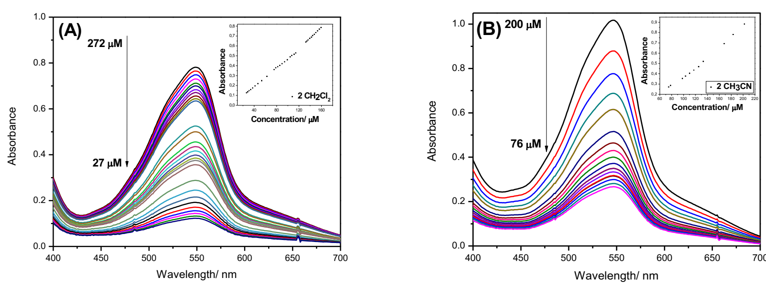

Fig. S6 UV-Vis of [Cu^{I}(*biq*)$_2$]ClO$_4$ at different concentrations. Inset: plot concentrations vs absorbance of all the concentrations used for the calculation of molar extinction coefficients λ_{max}: 549 nm. (A) in CH_2Cl_2, (B) in CH_3CN.

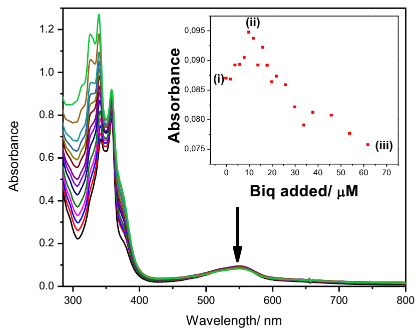

Fig. S7 UV-Vis spectra of $[Cu^{I}(biq)_2]ClO_4$ 1 x 10^{-5} M in presence of several biq concentrations in CH_2Cl_2 solvent with 0.1 M $TBAClO_4$. Inset: Plot of the absorbance at 549 nm (MLCT band) vs biq concentration. (i) Correspond to initial point, $[Cu^{I}(biq)_2]ClO_4$ only; (ii) Correspond to 1:1 relation between $[Cu^{I}(biq)_2]ClO_4$ and *biq*; (iii) Correspond to final point, *biq* excess.

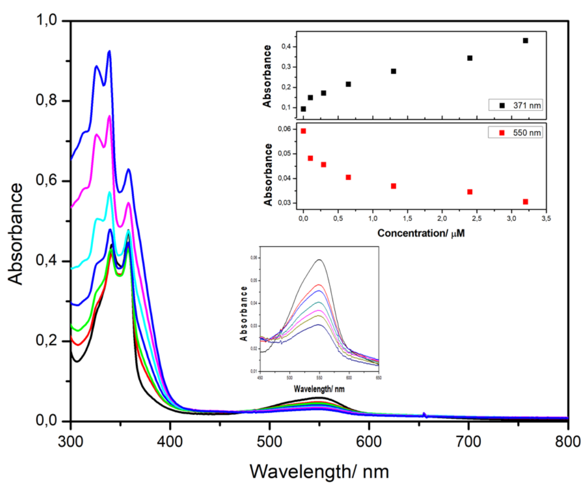

Fig. S8 UV-Vis spectra of $[Cu^{I}(biq)_2]ClO_4$, 1 x 10^{-5} M (A solution) with several concentrations of B solution (mixing between 1 x 10^{-5} M of {$[Cu^{I}(biq)_2]ClO_4$-biq} and 1 x 10^{-4} M of *biq)* in CH_2Cl_2 solvent. Inset: Plot of the absorbance at 550 nm (MLCT band) vs Concentration of A solution (red line) and Plot of the absorbance at 371 nm (intraligand band) vs Concentration of A solution (black line).

Comentado [NMA7]: New Figure added to S.I.

5. Synthesis and characterization of complexes

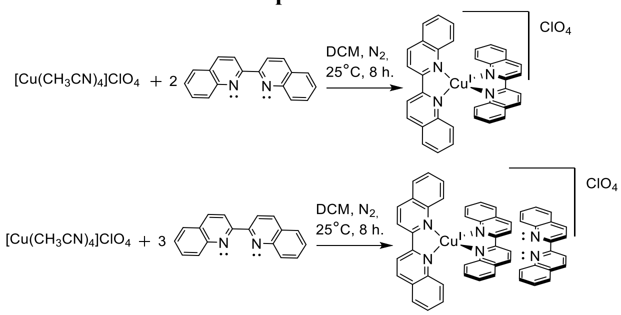

Fig. 9 Scheme of synthesis of {[Cu^{I}(*biq*)$_2$]ClO_4-*biq*} and [Cu(*biq*)$_2$]ClO_4.

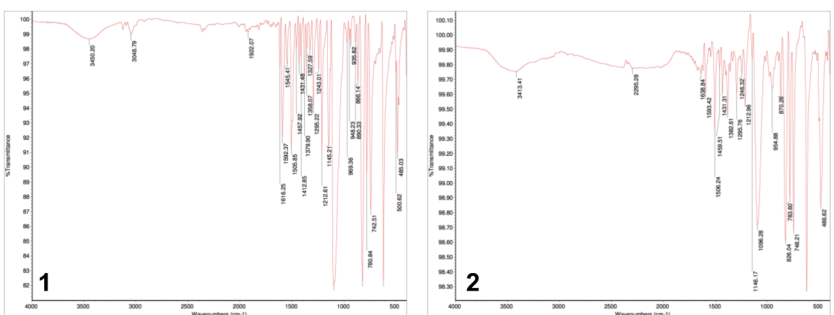

Fig. 10 IR spectra for complexes {[Cu^{I}(*biq*)$_2$]ClO_4-*biq*} (1) and [Cu(*biq*)$_2$]ClO_4 (2). Conditions: KBr pellet, FT-IR Nicolet iS10 spectrometer.

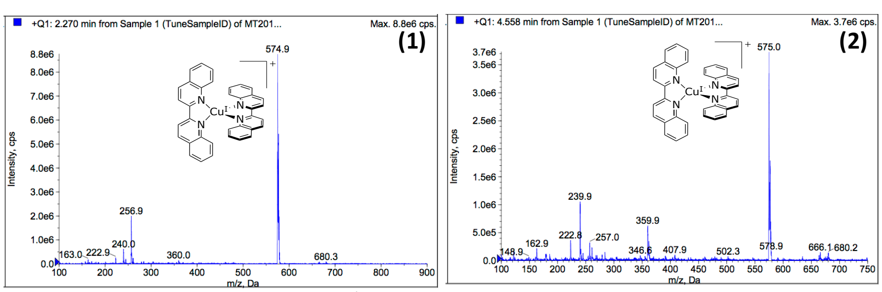

Fig. 11 Mass spectra for complexes {[Cu^{I}(*biq*)$_2$]ClO_4-*biq*} (**1**) and [Cu(*biq*)$_2$]ClO_4 (**2**). Conditions: CH_3CN solutions, AB SCIEX Triple QUAD 4500 spectrometer

116